Research Square

Preprints are preliminary reports that have not undergone peer review.
They should not be considered conclusive, used to inform clinical practice,
or referenced by the media as validated information.

Association Between Chest CT Features and Disease Severity in Children With Human Bocavirus Mono-infection: A Retrospective Cohort Study

Yilei Lao
Zhejiang University School of Medicine, National Clinical Research Center for Child Health
Luona Lin
Zhejiang University School of Medicine, National Clinical Research Center for Child Health
Yuhang Wu
Zhejiang University School of Medicine, National Clinical Research Center for Child Health
Lisu Huang
lisuhuang@zju.edu.cn

Zhejiang University School of Medicine, National Clinical Research Center for Child Health

Research Article

Keywords: human bocavirus, children, pneumonia, chest CT, disease severity

Posted Date: June 29th, 2026

DOI: https://doi.org/10.21203/rs.3.rs-9775653/v1

License: This work is licensed under a Creative Commons Attribution 4.0 International License.
Read Full License

Additional Declarations: No competing interests reported.

Version of Record: A version of this preprint was published at BMC Infectious Diseases on September 10th, 2026. See the published version at https://doi.org/10.1186/s12879-026-14339-7.

Abstract

Background

Human bocavirus (HBoV) is an established cause of pediatric lower respiratory tract infection, but the clinical relevance of chest CT findings in HBoV mono-infection remains uncertain.

Methods

We retrospectively studied hospitalized children (< 18 years) with PCR-confirmed HBoV mono-infection and LRTI between September 2022 and December 2023. Disease severity was classified as moderate, severe, or critical. Chest CT images were independently reviewed by two blinded pediatric radiologists. Associations between imaging findings and critical disease were evaluated using logistic regression. Viral genomic analysis was performed in a subset of patients.

Results

A total of 194 children were included, including 124 (63.9%) moderate, 46 (23.7%) severe, and 24 (12.4%) critical cases. GGO was the most common CT finding across all severity groups (> 90%) and showed no association with critical disease. In contrast, uneven lung inflation increased stepwise with severity (moderate, 24.2%; severe, 54.3%; critical, 66.7%; $P < 0.001$). Both uneven lung inflation and atelectasis were independently associated with critical illness after adjustment for age and sex (uneven lung inflation: adjusted OR, 3.74; 95% CI, 1.53–9.82; $P = 0.005$; atelectasis: adjusted OR, 3.51; 95% CI, 0.99–11.08; $P = 0.038$). Kaplan–Meier analysis further showed that uneven lung inflation was associated with longer hospitalization (log-rank $P = 0.048$), while atelectasis showed a similar but non-significant trend.

Conclusion

In children with PCR-confirmed HBoV mono-infection, GGO was consistently observed across all severity groups and showed no association with critical disease. In contrast, imaging features reflecting ventilation heterogeneity, particularly uneven lung inflation and atelectasis, were independently associated with critical illness after adjustment for age and sex. Kaplan–Meier analysis further demonstrated that uneven lung inflation was associated with prolonged hospitalization, with a similar but non-significant trend observed for atelectasis.

Introduction

Human bocavirus (HBoV), a member of the Parvoviridae family identified in 2005, is increasingly detected in young children with lower respiratory tract infection (LRTI), with reported prevalence ranging from 0.8% to 23% in pediatric cohorts [1, 2]. Although it was initially regarded as a bystander virus, more

recent studies using quantitative PCR and exclusion of co-infections support its role as a true respiratory pathogen capable of causing disease ranging from mild upper respiratory illness to severe pneumonia requiring intensive care [3, 4].

HBoV shows clear tropism for airway epithelial cells. Experimental models of human airway epithelium have demonstrated that infection disrupts epithelial integrity and induces airway-centered injury with associated inflammatory responses [5, 6]. These findings provide a biological basis for airway-predominant clinical manifestations, including wheezing, small airway obstruction, and ventilation heterogeneity. HBoV infection has also been associated with plastic bronchitis, in which endobronchial casts lead to acute airway obstruction and secondary atelectasis [7].

Despite these observations, CT manifestations of HBoV infection remain incompletely characterized. Previous imaging studies have mainly reported nonspecific findings such as ground-glass opacities (GGO) and consolidation, but are limited by small sample sizes, mixed infections, and lack of severity stratification [8]. As a result, imaging features that truly reflect clinically meaningful disease severity remain uncertain, particularly in immunocompetent children with confirmed mono-infection.

We therefore hypothesized that CT features reflecting ventilation heterogeneity and airway dysfunction would be more closely associated with disease severity than diffuse parenchymal abnormalities such as GGO. To test this, we analyzed chest CT findings in hospitalized children with PCR-confirmed HBoV mono-infection and assessed their association with clinical severity.

Methods

Study Design and Patient Cohort

This retrospective study included hospitalized children (< 18 years of age) with lower respiratory tract infection (LRTI) attributed to PCR-confirmed Human bocavirus mono-infection who were admitted to the Children's Hospital, Zhejiang University School of Medicine between September 2022 and December 2023.

Inclusion criteria were: (1) age < 18 years with clinical diagnosis of LRTI requiring hospitalization; (2) PCR-confirmed HBoV mono-infection; and (3) a final diagnosis of HBoV-associated LRTI established by attending pediatricians based on comprehensive clinical evaluation, with cases of sole HBoV detection further confirmed by expert consensus. Patients were excluded if they had (1) incomplete clinical or imaging data; (2) documented co-detection of other respiratory pathogens; or (3) repeated admission for the same infectious episode.

Disease severity was classified as moderate, severe, or critical according to institutional pediatric pneumonia criteria [9, 10]. Severe disease was defined by the presence of at least one of the following: cyanosis or hypoxemia; or radiological evidence of complications including pleural effusion, atelectasis, pneumothorax, emphysema, mediastinal emphysema, or pneumomediastinum; or extrapulmonary

involvement such as hepatic injury, myocardial injury, or seizures. Critical disease was defined by any of the following: pediatric Sequential Organ Failure Assessment (pSOFA) score ≥ 2, acute respiratory distress syndrome (ARDS), Glasgow Coma Scale (GCS) score ≤ 12, or oxygen saturation ≤ 90% despite oxygen therapy. Patients not meeting severe or critical criteria were classified as moderate.

The study protocol was conducted in accordance with the Declaration of Helsinki and was approved by the Ethics Committee of the Children's Hospital, Zhejiang University School of Medicine (IRB No. 2024-IRB-0384-P-01). Written informed consent was obtained from the guardians of all participants.

Clinical Data and Laboratory Measurements

Demographic characteristics, clinical features, treatment information, and outcomes were obtained from electronic medical records. Laboratory assessments included inflammatory and coagulation markers, including white blood cell count, C-reactive protein, and D-dimer, as well as cytokines, including interleukin (IL)-2, IL-4, IL-6, IL-10, tumor necrosis factor α (TNF-α), and interferon γ (IFN-γ). Chest computed tomography (CT) examinations performed during hospitalization were reviewed as part of the imaging analysis.

Chest CT Image Evaluation

Chest CT images were independently reviewed by 2 experienced pediatric radiologists who were blinded to clinical severity. Discrepancies were resolved by consensus review. Imaging findings were evaluated using predefined radiological criteria and included ground-glass opacity (GGO), consolidation, atelectasis, emphysema, mediastinal emphysema, uneven lung inflation, tracheobronchial stenosis, air bronchogram sign, pleural effusion, pleural thickening, cavity formation, and lobar involvement. In patients with uneven lung inflation, the lobar distribution of abnormalities was additionally recorded.

Viral Mutation Analysis

Whole-genome sequencing was performed on DNA from selected mono-infection samples using the Illumina NovaSeq 6000 platform. Sequencing reads were quality-filtered and assembled with CLC Genomics Workbench (version 23.0.3, Qiagen). Non-synonymous amino acid substitutions were identified, and mutation burden was defined as the total number of mutations per sample.

Statistical Analysis

Continuous variables are presented as median (interquartile range [IQR]), and categorical variables as number (%). Comparisons between groups were performed using the Kruskal–Wallis test, χ^2 test, or Fisher's exact test, as appropriate. Logistic regression analysis was used to estimate odds ratios (ORs) and 95% confidence intervals (CIs) for associations between CT imaging findings and critical disease.

Kaplan–Meier analysis with log-rank testing was performed to evaluate the association between imaging findings and duration of hospitalization. A two-sided P value 0 < 0.05 was considered statistically significant.

Results

Cohort Overview and Baseline Clinical Characteristics

A total of 194 immunocompetent children with PCR-confirmed HBoV mono-infection were included, comprising 124 moderate (63.9%), 46 severe (23.7%), and 24 critical cases (12.4%). The cohort was predominantly male (61.3%), with similar age and sex distributions among the three severity groups (Table 1). Cough was almost universal. Clinical manifestations associated with respiratory distress, including wheezing, cyanosis, shortness of breath, dyspnea, and three concave signs, became increasingly frequent as disease severity worsened (all $P < 0.01$). By comparison, the prevalence of rhonchi, rhinorrhea, fever, and fever duration did not differ significantly across groups. Escalation of treatment paralleled disease severity. Steroid use was substantially more common in critical illness than in moderate disease (87.5% vs. 33.9%, $P < 0.001$), and γ-globulin use also varied significantly among groups ($P = 0.049$). All ICU admissions were confined to the critical group. Length of hospital stay and viral DNA load were not significantly associated with disease severity. In addition, HBoV gene mutation frequency differed marginally between groups ($P = 0.050$). Baseline laboratory parameters are summarized in Supplementary Table 1.

Table 1
Clinical Characteristics of Hospitalized Children with HBoV Mono-Infection, Stratified by Disease Severity

Variable	Moderate(n = 124)	Severe(n = 46)	Critical(n = 24)	Total (n = 194)	*P*
Age					0.305
< 1 year, n (%)	20 (16.1)	11 (23.9)	6 (25.0)	37 (19.1)	
1–2 years, n (%)	38 (30.7)	16 (34.8)	10 (41.7)	64 (33.0)	
> 2 years, n (%)	66 (53.2)	19 (41.3)	8 (33.3)	93 (47.9)	
Male, n (%)	75 (60.5)	29 (63.0)	15 (62.5)	119 (61.3)	0.947
Symptoms					
Cough, n (%)	122 (98.4)	46 (100.0)	24 (100.0)	192 (99.0)	1.000
Wheezing, n (%)	60 (48.4)	30 (65.2)	20 (83.3)	110 (56.7)	0.003
Rhonchi, n (%)	6 (4.8)	4 (8.7)	2 (8.3)	12 (6.2)	0.548
Rhinorrhea, n (%)	39 (31.5)	11 (23.9)	3 (12.5)	53 (27.3)	0.136
Fever, n (%)	104 (83.9)	40 (87.0)	20 (83.3)	164 (84.5)	0.872
Fever days, median (IQR)	3.0 (2.0–4.0)	3.0 (2.0–3.0)	2.5 (2.0-3.3)	3.0 (2.0–4.0)	0.951
Cyanosis, n (%)	0 (0.0)	3 (6.5)	3 (12.5)	6 (3.09)	< 0.001
Shortness of breath, n (%)	33 (26.6)	23 (50.0)	19 (79.2)	75 (38.7)	< 0.001
Dyspnea, n (%)	7 (5.7)	5 (10.9)	11 (45.8)	23 (11.9)	< 0.001
Three concave signs, n (%)	23 (18.6)	16 (34.8)	15 (62.5)	54 (27.8)	< 0.001
Treatment					
Steroid use, n (%)	42 (33.9)	22 (47.8)	21 (87.5)	85 (43.8)	< 0.001
γ-globulin use, n (%)	3 (2.4)	3 (6.5)	3 (12.5)	9 (4.6)	0.049
ICU treatment, n (%)	0 (0.0)	0 (0.0)	9 (37.5)	9 (4.6)	< 0.001
Days of hospitalization, day, median (IQR)	5.0 (3.0–6.0)	5.0 (4.0–7.0)	6.0 (4.0–6.0)	5.0 (4.0–6.0)	0.161

Variable	Moderate(n = 124)	Severe(n = 46)	Critical(n = 24)	Total (n = 194)	*P*
Gene mutation rate, n/N (%)	33/124 (26.6)	5/46 (10.9)	8/24 (33.3)	46/194 (23.7)	0.050
Viral DNA load, median (IQR)	22100 (1107-262500)	71200 (2380-410000)	106850 (5542-820750)	27700 (1920-363000)	0.326

Data are presented as median (IQR) or n (%). Group comparisons across disease severity were performed using the Kruskal–Wallis test for continuous variables and the chi-square test or Fisher's exact test for categorical variables.

Chest CT Imaging Spectrum and Its Association with Disease Severity

Chest CT findings varied widely, and several imaging patterns were identified in HBoV infection (Fig. 1a). Ground-glass opacity (GGO) was the most common finding, seen in over 90% of cases. Uneven lung inflation was the second most frequent feature and the most distinctive abnormality apart from diffuse GGO. Lobar involvement was less common overall and most frequently involved the right middle, left upper, and right lower lobes. Tracheobronchial stenosis was observed in a small proportion of patients. Consolidation, atelectasis, air bronchogram sign, pleural effusion, and pleural thickening were less frequent overall, whereas emphysema, cavity formation, and mediastinal emphysema were uncommon. Representative CT findings in HBoV infection, including consolidation with air bronchogram sign, bilateral GGO, uneven lung inflation, pleural thickening, and pleural effusion, are shown in Fig. 2.

1. (A) Overall distribution of chest CT abnormalities in the full cohort.
2. (B) Distribution of imaging features stratified by disease severity (moderate, n = 124; severe, n = 46; critical, n = 24).

Data are expressed as n (%). Comparisons across groups were performed using the chi-square test or Fisher's exact test, as appropriate. Statistical significance is indicated as **P* < 0.05, ***P* < 0.01, ****P* < 0.001.

Representative CT images illustrating common radiological patterns of HBoV pneumonia: (A) uneven lung inflation; (B) consolidation; (C) air bronchogram sign; (D) mediastinal emphysema; (E) pleural thickening; and (F) pleural effusion. Lesions are indicated by red arrows.

When we broke down the findings by disease severity, clear trends appeared (Fig. 1b). GGO remained common across all groups (moderate, 92.7%; severe, 97.8%; critical, 87.5%; *P* = 0.185). In contrast, uneven lung inflation increased with disease severity, from 24.2% in moderate cases to 54.3% in severe and 66.7% in critical cases (*P* < 0.001). Atelectasis was absent in moderate cases but appeared more often in severe (23.9%) and critical (20.8%) cases (*P* < 0.001).

Consolidation ($P < 0.001$), emphysema ($P = 0.002$), pleural effusion ($P < 0.001$), and mediastinal emphysema were observed mainly in severe and critical cases. The air bronchogram sign was more common in severe cases (17.4%) but was not observed in critical cases ($P = 0.003$). Lobar involvement also tended to occur more frequently in severe and critical disease, particularly in the left upper, right middle, and right lower lobes. Tracheobronchial stenosis, cavity formation, and pleural thickening showed no significant differences across severity groups (all $P > 0.05$). Representative CT images demonstrate the spectrum of pulmonary abnormalities in HBoV infection (Fig. 2). Uneven lung inflation is seen as patchy, heterogeneous aeration with alternating areas of reduced and relatively preserved inflation (Fig. 2a). Consolidation appears as focal or segmental increased attenuation with blurred vascular margins (Fig. 2b). Air bronchograms are present within consolidated areas, reflecting air-filled bronchi surrounded by alveolar opacification (Fig. 2c). Mediastinal emphysema is characterized by streaky low-attenuation air tracking along mediastinal structures (Fig. 2d). Pleural thickening manifests as localized pleural-based linear or band-like high-density lesions (Fig. 2e), while pleural effusion appears as dependent fluid accumulation in the pleural space (Fig. 2f). Red arrows denote the corresponding imaging features in each panel. Uneven lung inflation and atelectasis were the imaging features most strongly associated with worsening disease severity.

CT Imaging Findings and Risk of Critical Disease

Logistic regression analyses were performed to assess the association between chest CT features and critical disease in the total cohort (Table 2). After adjustment for age and sex, uneven lung inflation was independently associated with critical disease (adjusted OR, 3.74; 95% CI, 1.53–9.82; $P = 0.005$). Atelectasis also showed a significant association in the adjusted model (adjusted OR, 3.51; 95% CI, 0.99–11.08; $P = 0.038$). In contrast, GGO, consolidation, emphysema, tracheobronchial stenosis, and lobar involvement were not significantly associated with critical disease in either univariate or multivariate analyses. Air bronchogram sign was identified only in non-critical patients. Uneven lung inflation occurred more frequently in critically ill patients, resulting in complete or quasi-complete separation that prevented reliable estimation of odds ratios for some comparisons.

Odds ratios (ORs) and 95% confidence intervals (CIs) were derived from univariate and multivariate logistic regression models assessing associations between CT imaging features and critical disease. Multivariate analyses were adjusted for age and sex. “Critical/Absent” and “Critical/Present” indicate the number of patients who developed critical illness among those without or with the corresponding imaging feature. NE denotes not estimable due to complete or quasi-complete separation. All statistical tests were two-sided

Kaplan–Meier analysis showed that uneven lung inflation was associated with longer hospitalization (log-rank P = 0.048) (Fig. 3a). Median hospital stay was estimated at 14 days in patients with uneven lung inflation, while the median was not reached in those without uneven lung inflation during the observation period. Atelectasis showed a similar trend but did not reach statistical significance (log-rank $P = 0.088$) (Fig. 3b). Patients with atelectasis had an estimated median hospital stay of 14 days, while the median duration was not reached in those without atelectasis. These findings were consistent with

the regression analyses and further supported the association between uneven lung inflation and more severe clinical outcomes.

Shaded areas represent 95% confidence intervals, and tick marks indicate censored observations.

Discussion

Respiratory viruses remain a major cause of pediatric pneumonia and hospitalization worldwide [11, 12]. HBoV is increasingly recognized as a cause of pediatric lower respiratory tract infection (LRTI) [13–15]. Experimental and in vitro studies have demonstrated that HBoV preferentially infects airway epithelium and induces epithelial injury with associated inflammatory responses [16]. These observations support an airway-centered disease mechanism, with potential manifestations ranging from bronchitis and bronchiolitis to more extensive parenchymal involvement [17, 18]. However, radiological correlates of these pathogenic processes in clinical cohorts remain insufficiently defined.

In the present study, GGO was observed in the majority of patients regardless of severity status, indicating that this abnormality likely represents a common feature of viral lung involvement rather than a marker of critical disease. Uneven lung inflation, by contrast, showed a clear association with disease severity, increasing progressively from moderate to critical disease. Atelectasis was observed predominantly in severe and critical cases and remained independently associated with critical illness after adjustment for age and sex. These findings indicate that imaging abnormalities related to ventilation heterogeneity and airway dysfunction may be more closely linked to severe clinical presentation than diffuse parenchymal abnormalities alone.

Compared with previous imaging studies of HBoV infection, our findings show both concordance and notable differences. Earlier reports have predominantly described bilateral GGO and patchy consolidation as the most frequent CT abnormalities in children with HBoV-associated LRTI, often without clear stratification by disease severity or infection status [19, 20]. In several of these studies, mixed viral infections were common, and imaging findings were interpreted primarily as nonspecific viral pneumonia patterns [21, 22]. In contrast, our cohort was restricted to PCR-confirmed mono-infection in immunocompetent children, which reduces confounding from co-pathogens and may better reflect the intrinsic radiological phenotype of HBoV infection. Under these conditions, we observed that GGO was highly prevalent across all severity groups and showed limited value in distinguishing severe disease, whereas airway-related abnormalities such as uneven lung inflation and atelectasis showed stronger and more consistent associations with clinical severity. These findings raise the possibility that diffuse parenchymal abnormalities represent shared features of viral pneumonia, whereas airway-related dysfunction may play a more prominent role in severe HBoV infection.

Mechanistically, uneven lung inflation likely reflects heterogeneous small airway obstruction, whereas atelectasis may represent more advanced or persistent ventilation impairment [23]. The parallel increase in dyspnea, shortness of breath, and three concave signs across severity groups further supports the clinical relevance of airway-centered ventilatory dysfunction in severe HBoV infection. The progressive increase of these findings across severity strata supports a pathophysiological model in which airway

injury and obstruction, rather than diffuse alveolar involvement alone, contribute to clinical deterioration. Consistent with this interpretation, Kaplan–Meier analysis demonstrated prolonged hospitalization in patients with uneven lung inflation, further supporting its clinical relevance as a marker of disease burden. Additional imaging abnormalities, including consolidation, emphysema, pleural effusion, and mediastinal emphysema, were observed mainly in severe and critical cases, suggesting more extensive pulmonary injury in advanced disease. However, these features were not independently associated with critical illness after adjustment, possibly reflecting their occurrence as secondary or downstream manifestations of severe airway disease rather than primary drivers of severity. Air bronchogram sign was identified only in non-critical patients, although the limited number of cases precludes firm interpretation.

Overall, our findings suggest that CT abnormalities related to ventilation heterogeneity and airway dysfunction may be more informative for assessing disease severity than GGO alone. Chest CT is unlikely to be necessary in uncomplicated HBoV infection, but may be useful in patients with marked respiratory distress or worsening clinical status..

Limitations

Several limitations should be considered. First, this was a retrospective single-center study, which may limit the generalizability of the findings. Second, despite restricting the cohort to children with PCR-confirmed HBoV mono-infection, the possibility of undetected co-infection cannot be excluded completely. Third, CT acquisition protocols were not completely standardized, which may have influenced detection of subtle imaging abnormalities. The number of critical cases was relatively small, and some imaging findings were uncommon, which reducing statistical power in subgroup analyses. Laboratory markers were measured only once during hospitalization, precluding assessment of longitudinal changes.

Strengths and Future Directions

This study focused specifically on immunocompetent hospitalized children with PCR-confirmed HBoV mono-infection, a population that remains insufficiently characterized in previous imaging studies. The inclusion of patients across moderate, severe, and critical disease categories enabled assessment of CT abnormalities across a broad clinical spectrum. In addition, the combined use of logistic regression and Kaplan–Meier analyses allowed evaluation of both disease severity and hospitalization course in relation to imaging findings.

Future multicenter studies with standardized imaging protocols are needed to validate these findings in larger cohorts. Longitudinal studies incorporating serial imaging and repeated biomarker measurements may further clarify the temporal evolution of airway-centered abnormalities during severe disease. Additional investigation is also warranted to determine whether specific viral mutations are reproducibly associated with distinct imaging phenotypes or clinical outcomes.

Conclusion

In hospitalized children with HBoV mono-infection, GGO was highly prevalent across all severity groups and was not associated with critical disease. By contrast, uneven lung inflation and atelectasis showed stronger associations with severe clinical presentation, and uneven lung inflation was additionally associated with prolonged hospitalization. Other abnormalities, including consolidation, pleural effusion, emphysema, and mediastinal emphysema, were observed predominantly in severe and critical cases but were not independently associated with critical illness after adjustment. Overall, these findings suggest that CT features reflecting airway dysfunction and uneven ventilation may provide greater clinical relevance for severity assessment than diffuse GGO alone in pediatric HBoV infection.

Abbreviations

HBoV	Human bocavirus
LRTI	Lower respiratory tract infection
PCR	Polymerase chain reaction
CT	Computed tomography
GGO	Ground-glass opacity
OR	Odds ratio
CI	Confidence interval
IQR	Interquartile range
IL	Interleukin
TNF-α	Tumor necrosis factor alpha
IFN-γ	Interferon gamma
pSOFA	Pediatric Sequential Organ Failure Assessment
ARDS	Acute respiratory distress syndrome
GCS	Glasgow Coma Scale

Declarations

Acknowledgments

The study investigators and coordinators gratefully acknowledge all study participants.

Funding

This work was supported by National Natural Science Foundation of China (82073561) and the Key Program of The Independent Design Project of National Clinical Research Center for Children and Adolescents' Health and Diseases (No. G25C0001).

Conflicts of interest

All authors declare that they have no competing interests regarding this manuscript.

References

1. Fernando TN, Dayananda D, Muthugala R. Human bocavirus: As an emerging respiratory pathogen. World J Virol. 2025;14(4). 10.5501/wjv.v14.i4.115043.
2. Jalving HT, Heimdal I, Valand J, Risnes K, Krokstad S, Nordbø SA, et al. The Burden of Human Bocavirus 1 in Hospitalized Children With Respiratory Tract Infections. J Pediatr Infect Dis Soc. 2023;12(5):282–9. 10.1093/jpids/piad027.
3. Tan J, Huang Z, Tang W, Liu G, Li P, Wen J et al. Human bocavirus-1 infection in hospitalized pediatric patients with acute respiratory tract infections. Liu BM, editor. Microbiol Spectr. 2025;13(4):e02985-24. 10.1128/spectrum.02985-24
4. Xu M, Arku B, Jartti T, Koskinen J, Peltola V, Hedman K, et al. Comparative Diagnosis of Human Bocavirus 1 Respiratory Infection With Messenger RNA Reverse-Transcription Polymerase Chain Reaction (PCR), DNA Quantitative PCR, and Serology. J Infect Dis. 2017;215(10):1551–7. 10.1093/infdis/jix169.
5. Yan Z, Deng X, Qiu J. Human Bocavirus 1 Infection of Well-Differentiated Human Airway Epithelium. Curr Protoc Microbiol. 2020;58(1):e107. 10.1002/cpmc.107 . PubMed PMID: 32639683; PubMed Central PMCID: PMC7422954.
6. Deng X, Zou W, Xiong M, Wang Z, Engelhardt JF, Ye SQ et al. Human Parvovirus Infection of Human Airway Epithelia Induces Pyroptotic Cell Death by Inhibiting Apoptosis. Jung JU, editor. J Virol. 2017;91(24):e01533-17. 10.1128/JVI.01533-17
7. Fei-Zhou Z, Mei-Xia H, Xiaofen T, Lei W, Xuan J, Lan-Fang T. Plastic bronchitis associated with human bocavirus 1 infection in children. Pediatr Pulmonol. 2024;59(11):2754–60. 10.1002/ppul.27113.
8. Lee HN, Koo HJ, Kim SH, Choi SH, Sung H, Do KH. Human Bocavirus Infection in Adults: Clinical Features and Radiological Findings. Korean J Radiol. 2019;20(7):1226–35. 10.3348/kjr.2018.0634 . PubMed PMID: 31270986; PubMed Central PMCID: PMC6609429.
9. Christensen A, Kesti O, Elenius V, Eskola AL, Døllner H, Altunbulakli C, et al. Human bocaviruses and paediatric infections. Lancet Child Adolesc Health. 2019;3(6):418–26. 10.1016/S2352-4642(19)30057-4.
10. Tătăranu E, Galos F, Anchidin-Norocel L, Axinte R, Filip F, Axinte S, et al. Life-Threatening Conditions in Children with Bocavirus Infection-Case Series and Mini Review of the Literature. Viruses.

2024;16(9):1347. 10.3390/v16091347 . PubMed PMID: 39339824; PubMed Central PMCID: PMC11435620.

11. Rayamajhi Thapa R, Nascimento-Carvalho C, Allander T, Jartti T, Söderlund-Venermo M. A Diagnostic Approach to Separate Acute Human Bocavirus 1 Respiratory Tract Infection From Long-lasting Virus Shedding. J Infect Dis. 2025;231(5):e862–6. 10.1093/infdis/jiaf130 . PubMed PMID: 40079329; PubMed Central PMCID: PMC12128058.
12. McAllister DA, Liu L, Shi T, Chu Y, Reed C, Burrows J, et al. Global, regional, and national estimates of pneumonia morbidity and mortality in children younger than 5 years between 2000 and 2015: a systematic analysis. Lancet Glob Health. 2018;7(1):e47–57. (18)30408-X PubMed PMID: 30497986; PubMed Central PMCID: PMC6293057.
13. Lin L. Severe Lower Respiratory Tract Infection in Patients With Human Bocavirus Monoinfection in Southeast China.
14. Arnold JC, Singh KK, Spector SA, Sawyer MH. Human Bocavirus: Prevalence and Clinical Spectrum at a Children's Hospital. Clin Infect Dis Off Publ Infect Dis Soc Am. 2006;43(3):283–8. doi:10.1086/505399 PubMed PMID: 16804840; PubMed Central PMCID: PMC7107867.
15. Schildgen O, Müller A, Allander T, Mackay IM, Völz S, Kupfer B, et al. Human Bocavirus: Passenger or Pathogen in Acute Respiratory Tract Infections? Clin Microbiol Rev. 2008;21(2):291–304. 10.1128/CMR.00030-07 . PubMed PMID: 18400798; PubMed Central PMCID: PMC2292574.
16. Deng X, Zou W, Xiong M, Wang Z, Engelhardt JF, Ye SQ, et al. Human Parvovirus Infection of Human Airway Epithelia Induces Pyroptotic Cell Death by Inhibiting Apoptosis. J Virol. 2017;91(24):e01533–17. 10.1128/JVI.01533-17 . PubMed PMID: 29021400; PubMed Central PMCID: PMC5709578.
17. Stefanidis K, Konstantelou E, Yusuf GT, Oikonomou A. Et. A. Radiological, epidemiological and clinical patterns of pulmonary viral infections. Eur J Radiol. 2021. 10.1016/j.ejrad.2021.109548.
18. Ko JP, Girvin F, Moore W, Naidich DP. Approach to Peribronchovascular Disease on CT. Semin Ultrasound CT MR. 2019;40(3):187–99. 10.1053/j.sult. 2018.12.002 PubMed PMID: 31200868; PubMed Central PMCID: PMC7126938.
19. Liao J, Yang Z, He Y, Wei J, Ren L, Liu E, et al. Respiratory tract infection of fatal severe human bocavirus 1 in a 13-month-old child: A case report and literature review. Front Pediatr. 2022;10:949817. 10.3389/fped.2022.949817 . PubMed PMID: 36605757; PubMed Central PMCID: PMC9808049.
20. Liao J, Yang Z, He Y, Wei J, Ren L, Liu E, et al. Clinical characteristics and risk factors of severe bocavirus-positive pneumonia in children and a literature review. Pediatr Discov. 2025;3(4):e2523. 10.1002/pdi3. 2523 PubMed PMID: 41476735; PubMed Central PMCID: PMC12753018.
21. Tan J, Huang Z, Tang W, Liu G, Li P, Wen J et al. Human bocavirus-1 infection in hospitalized pediatric patients with acute respiratory tract infections. Liu BM, editor. Microbiol Spectr. 2025;13(4):e02985-24. 10.1128/spectrum.02985-24
22. Calvo C, García-García ML, Pozo F, Carballo D, Martínez-Monteserín E, Casas I. Infections and coinfections by respiratory human bocavirus during eight seasons in hospitalized children. J Med

Virol. 2016;88(12):2052–8. 10.1002/jmv.24562 . PubMed PMID: 27124519; PubMed Central PMCID: PMC7166349.

23. Hogg JC, Paré PD, Hackett TL. The Contribution of Small Airway Obstruction to the Pathogenesis of Chronic Obstructive Pulmonary Disease. Physiol Rev. 2017;97(2):529–52. 10.1152/physrev.00025.2015.

Table 2

Table 2 is available in the Supplementary Files section.

Figures

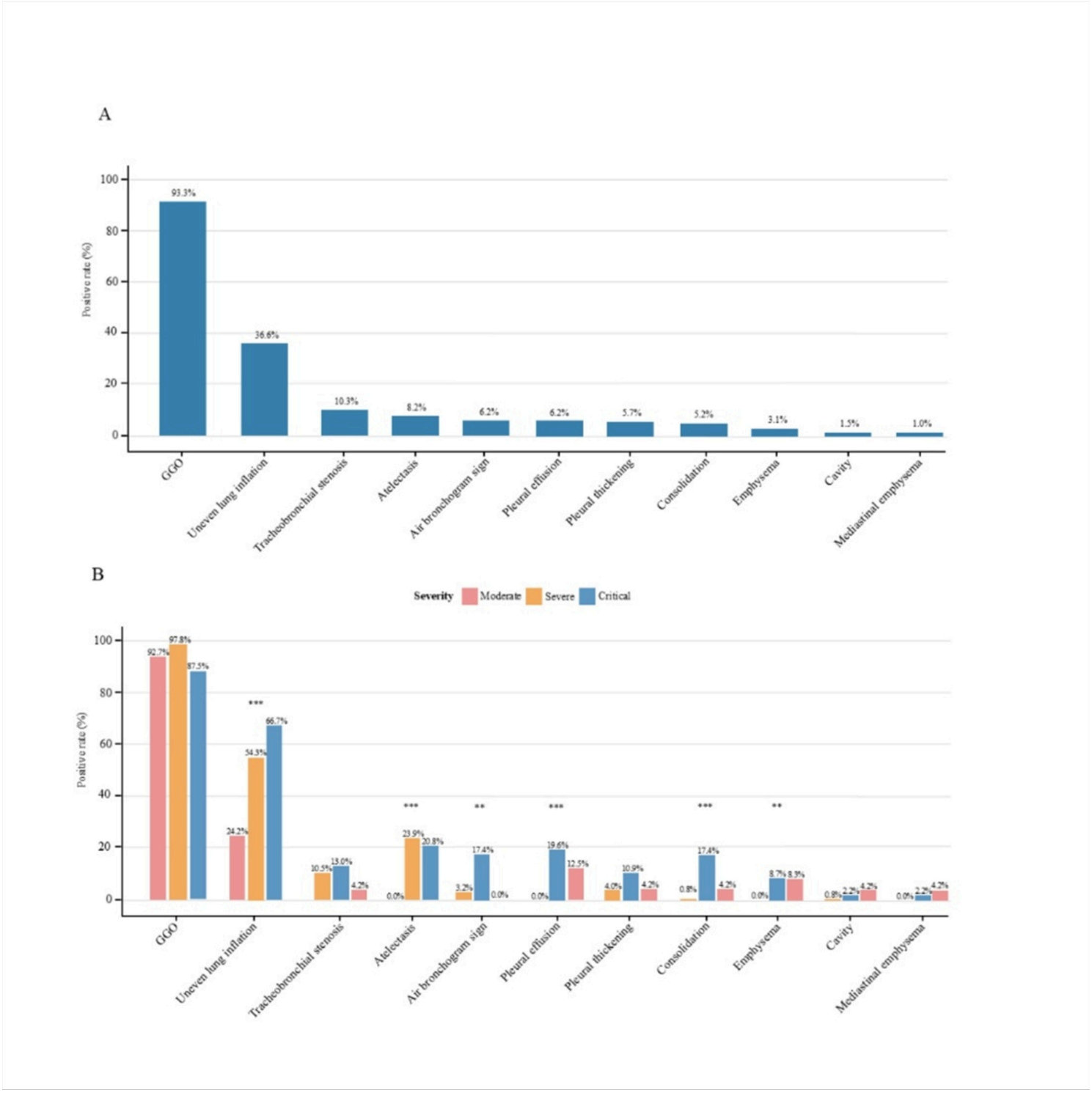


Figure 1

Chest CT imaging features in hospitalized children with human bocavirus infection (N = 194).

(A) Overall distribution of chest CT abnormalities in the full cohort.

(B) Distribution of imaging features stratified by disease severity (moderate, n = 124; severe, n = 46; critical, n = 24).

Data are expressed as n (%). Comparisons across groups were performed using the chi-square test or Fisher's exact test, as appropriate. Statistical significance is indicated as *$P < 0.05$, **$P < 0.01$, ***$P < 0.001$.

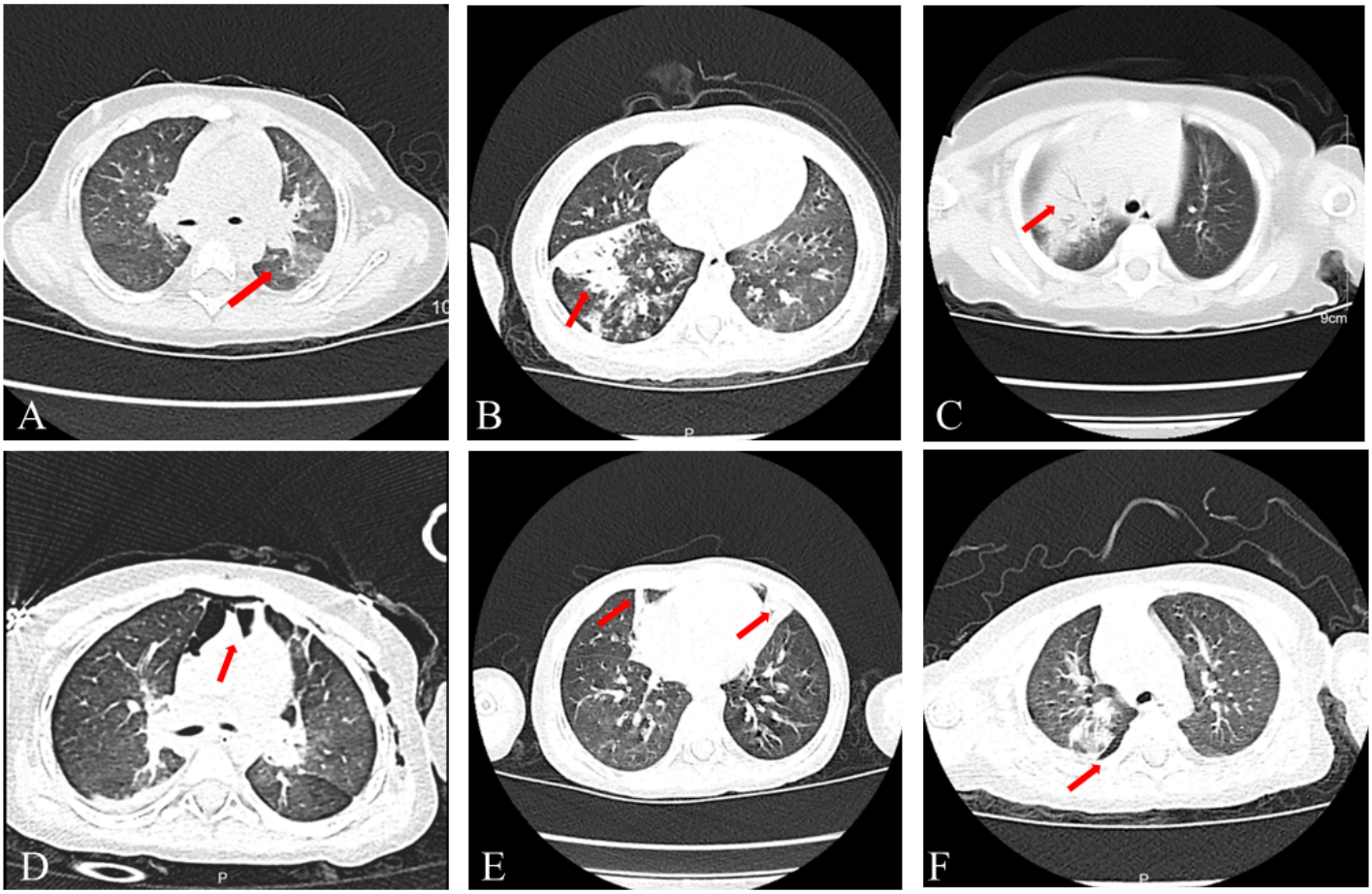


Figure 2

Representative chest CT findings in children with human bocavirus infection.

Representative CT images illustrating common radiological patterns of HBoV pneumonia: (A) uneven lung inflation; (B) consolidation; (C) air bronchogram sign; (D) mediastinal emphysema; (E) pleural thickening; and (F) pleural effusion. Lesions are indicated by red arrows.

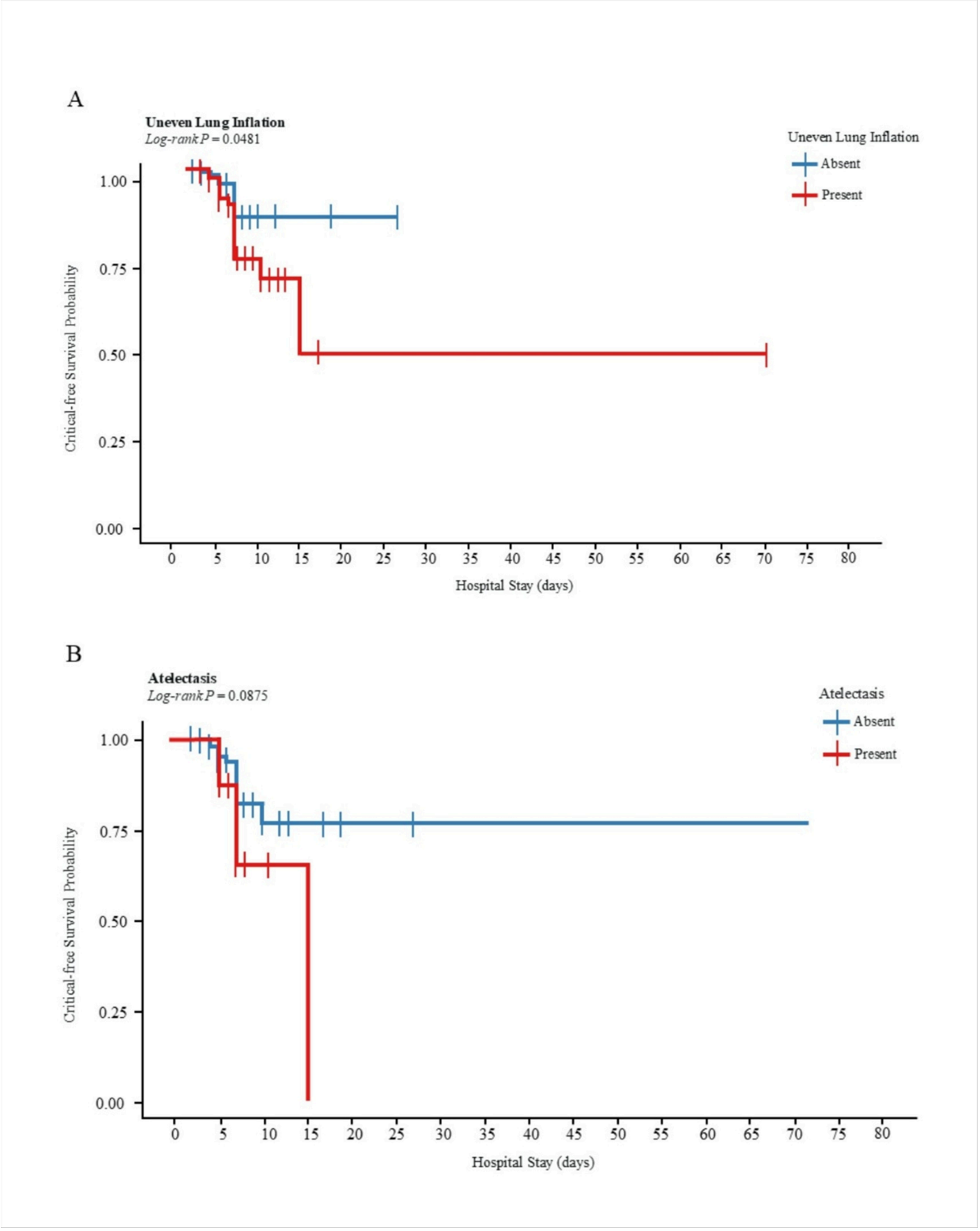


Figure 3

Kaplan–Meier curves for critical-free survival according to chest CT findings.

(A) Patients with uneven lung inflation (n = 71) showed shorter critical-free survival compared with those without (n = 123) (log-rank *P* = 0.048), with an estimated median time to critical illness of 14 days versus not reached.

(B) Patients with atelectasis (n = 16) demonstrated a trend toward reduced critical-free survival compared with those without (n = 177), although this did not reach statistical significance (log-rank *P* = 0.088).

Shaded areas represent 95% confidence intervals, and tick marks indicate censored observations.

Supplementary Files

This is a list of supplementary files associated with this preprint. Click to download.

- Supplementarymaterial.docx
- Table2.docx